PERGAMON

International Journal of Heat and Mass Transfer 46 (2003) 921–929

International Journal of HEAT and MASS TRANSFER

www.elsevier.com/locate/ijhmt

Simulation of the microstructure of a thin metal layer quenched from a liquid state

A.I. Fedorchenko *, A.A. Chernov

S.S. Kutateladze Institute of Thermophysics, Siberian Branch of the Russian Academy of Sciences, Novosibirsk 630090, Russia

Received 17 January 2002

Abstract

In the paper, the solidification of a thin metal layer on quenching from a liquid state is considered. The conditions of the glass transition of the melt are considered. Based on these conditions, the thickness of the metal glass sublayer adjoint to the backing is determined. The proposed model of spontaneous crystallization of the melt allows calculation of the grain size distribution in the cross-section of the layer. It also predicts the variation in the size of the grains in the layer quenched on different backings.

1. Introduction

At the present time, the methods of quenching from a liquid state are the basic methods for obtaining nonequilibrium structures such as metallic glasses, nano- and microcrystalline structures, quasicrystals, supersaturated solid solutions, etc. [1–4]. The main of these is the method of gas thermal deposition [5,6] based on the interaction of the drops of a melt with a backing and with the preliminarily coated layers and also the method of spinning when a thin layer of melt is poured onto a backing. In either of the cases, very high rates of cooling are realized (above 10^6 K/s), therefore the melt can solidify at considerable overcoolings which may attain 100–300 K. Moreover, there is an appreciable cooling rate gradient over the thickness of the quenched layer, i.e., the rates of cooling directly in the zone of contact of the melt with the backing and on the free surface of the melt may differ two orders of magnitude. This also results in a substantial inhomogeneity in the structure of the quenched layer over its thickness. This is excellently illustrated in [7], in which a 280-μm-thick coating consisting of several layers of deposited powder particles was obtained in plasma deposition of $ZrSiO_4$ powder. A foil was prepared from the coating-base cross-section for transmission electron microscopy. The phase composition of the layer was determined with the aid of X-ray diffraction. Investigations of the cross-sectional thin section have shown that the coating layer directly adjoining the base can be subdivided into several structural types: microcrystalline regions of ZrO_2 with small grains of size 25–50 nm and large grains of size 50–100 nm: the ZrO_2 grains ordered into the bands separated by an amorphous phase and a crystalline residue several orders of magnitude larger. The existence of the amorphous phase was confirmed by means of X-ray diffraction and it has been identified as SiO_2. Its greatest amount was found in the first deposited layer, but it was also detected in further layers of the base. This work convincingly showed that with distance from the base the phase composition of the layer changes substantially and passes successively from an amorphous and microcrystalline phases to a purely crystalline one.

These experimental facts point to the fact that the model of solidification of thin layers of the melt must necessarily include a stage of nonequilibrium phase transition. Thus, in crystallization of relatively thick layers the conditions of equilibrium solidification described by the Stephan model may realize. However, on decrease in the thickness of the layer or near the backing the mechanisms of equilibrium and nonequilibrium solidification begin to compete and, within the limit of

* Corresponding author. Tel.: +886-2-3366-5649; fax: +886-2-2363-9290.

E-mail address: fedor@spring.iam.ntu.edu.tw (A.I. Fedorchenko).

0017-9310/03/$ - see front matter
PII: S0017-9310(02)00350-2

Nomenclature

a	thermal diffusivity
$a_{b,m}$	dimensionless thermal diffusivity, a_b/a_m
a_c	radius of a critical nucleus, $2\sigma T_{mel}/(L_v \Delta T)$
c	specific heat
C	parameter, Eq. (3)
d_a	diameter of the atom
f	dimensionless function of the source, Eq. (9)
k_B	Boltzmann constant
K	kinetic coefficient
K_ε	relative thermal activity
Ku	Kutateladze number
h	Planck constant
h_g	amorphous sublayer thickness
h_m	thickness of the quenched layer
J	nucleation frequency
J_s	stationary nucleation frequency
L	specific heat of phase change
L_v	volumetric heat of phase change
M	number of nodes in the time interval $[0,1]$
N	number of nodes in the melt layer
N_1	number of nodes in a backing
N_a	number of atoms per unit volume
N_c	number of crystallization centers
r	radius of crystallite
q	rate of cooling
Q	quantity of heat released in the process of crystallization by spontaneously occurring new phase centers
t	time
t_{cr}	time of melt layer crystallization
t_g	time of melt cooling to glass formation temperature
t_R	time of molecular relaxation
t_{R0}	pre-exponential multiplier in the Arrhenius dependence of the time of molecular relaxation on temperature
T	temperature
T_g	temperature of glass formation
T_{mel}	melting temperature of the melt substance
ΔT	overcooling of the melt, $T_{mel} - T$
U	activation energy
v	rate of growth of a crystal
V	volume
V_g	volume of amorphizing substance
z	coordinate

Greek symbols

β	heat transfer coefficient at the phase change front
ζ	dimensionless coordinate, z/h_m
η	fraction of a crystalline phase
θ	dimensionless temperature, T/T_p^0
θ_m	dimensionless melting temperature of the melt substance, T_m/T_m^0
Θ	dimensionless temperature, Eq. (4)
λ	heat conduction coefficient
$\lambda_{b,m}$	dimensionless thermal conductivity, λ_b/λ_m
ρ	density
σ	surface tension at the melt–crystal interface
τ	dimensionless time, $a_m t/h_m^2$
τ_{cr}	dimensionless time of crystallization
Ω	criterion determining a priori the mechanism of consecutive phase transition: equilibrium or nonequilibrium, $\beta/(L_v K)$

Subscripts

b	refers to backing
i	number of the spatial sublayer
j	number of the time sublayer
m	refers to the melt layer

Superscripts

liq	refers to liquid phase
s	refers to solid phase
0	refers to initial state

very thin layers, purely nonequilibrium solidification becomes prevailing. Here, however, the following fact is to be noted. The degree of the departure of the solidification process from the equilibrium one due to the supercooling at the crystallization front depends not only on the thickness of the cooled layer, but also on external conditions as well as on the kinetic and thermophysical properties of the melt.

In [8] it is shown that for thin enough layers obtained on collision of a drop of the melt with the backing under the conditions close to the conditions of gaseous thermal deposition the solidification may follow both equilibrium and nonequilibrium mechanisms. The scenario of the phase transition (equilibrium or nonequilibrium) is determined by the criterion introduced in [8], i.e., $\Omega = \beta/(L_v K)$, where β is the coefficient of heat transfer at the phase change point; L_v is the volumetric heat of crystallization; K is the kinetic coefficient which depends on the properties of the melt. For the case of equilibrium crystallization there corresponds the condition $\Omega \ll 1$.

However, even though this criterion allows a priori prediction and optimization of the regime of solidification on collision of a drop of the melt with the backing, nevertheless the model of successive nonequilibrium phase transition which underlies the derivation of this criterion does not allow one to predict the microstructure of the layer obtained. Therefore, an attempt has been made in this work to carry out a detailed simula-

tion of the microstructure of a solidifying layer of the melt involving the elucidation of all the structural components, viz., the possibility of formation of an amorphous layer near the backing and determination of its thickness, and also, based on the model of spontaneous crystallization, determination of the size distribution of grains in the cross-section of the layer.

2. Amorphization of the melt

As noted in Section 1, when the melt is solidified near the backing, a thin amorphous sublayer is formed, the thickness of which can be found from the following considerations.

Let us formulate the conditions of the transition into glass of the melt in quenching [9]. First, in the process of cooling the temperature of the melt T_m must turn to be lower than the glass transition temperature T_g:

$$T_m \leqslant T_g, \tag{1}$$

which, according to the Bartenev–Rithland equation $qt_R(T_g) = k_B T_g^2/U$, is the function of the rate of cooling q [10]. Here $t_R(T) = t_{R0}\exp(U/k_B T)$ is the time of molecular relaxation; U is the activation energy; and k_B is the Boltzmann constant. The pre-exponential factor t_{R0} is determined from the relation $t_R(T_{mel}) = h/(k_B T_{mel})$, where h is the Planck constant; T_{mel} is the melting temperature of the melt. It follows from the Bartenev–Rithland equation that the glass transition temperature increases with increase in the rate of cooling.

Second, in the process of the cooling of the melt to the glass transition temperature, nuclei of the crystalline phase should not appear in the volume [11]:

$$V_g \int_0^{t_g} J(t)\,\mathrm{d}t < 1, \tag{2}$$

where V_g is the volume of an amorphizing melt; usually it is assumed [11] that $V_g = h_g^3$, h_g is the thickness of the amorphous layer; t_g is the time of the cooling of the melt to the glass transition temperature (at the moment of time t_g the melt is amorphized); $J(t)$ is the frequency of nucleation which is determined according to the results obtained in [12]:

$$J(t) = J_s \exp\left(-\frac{a_c}{12 d_a}\frac{t_R}{t}\right).$$

Here,

$$J_s = N_a C \exp\left(-\frac{U}{k_B t}\right)\exp\left(-\frac{16\pi}{3}\frac{\sigma^3 T_m^2}{L_v^2 \Delta T^2 k_B T}\right), \tag{3}$$

$\Delta T = T_{mel} - T$ is the overcooling of the melt; N_a is the number of the atoms (molecules) per unit volume; d_a is the diameter of the atom; σ is the surface tension at the melt–crystal interface; $a_c = 2\sigma T_{mel}/(L_v \Delta T)$ is the radius of the critical nucleus; $C = (2d_a/h)(\sigma k_B T)^{1/2}$. Here, J_s is the stationary frequency of nucleation which corresponds to the stationary process of phase transition (for $t \gg t_R$).

The rate of melt cooling q will be found from the solution of a conjugate problem of heat exchange of the layer of finite thickness brought into contact with a semi-infinite backing. The z-axis with the origin on the free surface of the layer is directed inside the backing. Then, according to the results obtained in [13] the temperature field $T(t,z)$ behaves as follows:

$$T(t,z) = T_b^0 + (T_m^0 - T_b^0)\Theta(t,z).$$

Here,

$$\Theta(t,z) = 1 - \frac{1}{1+K_\varepsilon}\sum_{n=1}^{\infty}(-\alpha)^{n-1} \times \left\{\operatorname{erfc}\left(\frac{(2n-1)h_m - z}{2\sqrt{a_m t}}\right) + \operatorname{erfc}\left(\frac{(2n-1)h_m + z}{2\sqrt{a_m t}}\right)\right\}, \tag{4}$$

T_m^0 and T_b^0 is the initial temperature of the melt and of the backing, respectively; h_m is the thickness of the melt layer; $\alpha = (1-k_\varepsilon)/(1+k_\varepsilon)$, $k_\varepsilon = \sqrt{\lambda_m \rho_m c_m/(\lambda_b \rho_b c_b)}$ is the relative thermal activity: ρ, c, λ, and a are the density, heat capacity, thermal conductivity, and thermal diffusivity; the subscripts m and b correspond to the material of the melt and backing. The formula for the rate of cooling the layer $q(t,z) = -\mathrm{d}T(t,z)/\mathrm{d}t$ is not given here because of its unwieldiness. We note that the rate of cooling depends on the coordinate z.

The calculations carried out for the layers of thickness $h_m \sim 1$ μm have shown that amorphization conditions (1) and (2) are satisfied only for a thin sublayer near the backing: $h_m - h_g \leqslant z \leqslant h_m$. This is explained by the fact that the rate of cooling of the melt $q(t,z)$ near the backing at the initial time instant is much higher than far from it. The results of calculations of the amorphous sublayer thickness in the case of quenching of an aluminum, a copper, and a nickel layers of the melt of thickness 1 μm on a copper backing are presented in Table 1. All the thermophysical and kinetic properties of substances used in the calculations are listed in Table 2; the superscripts s and liq correspond to a solid and a liquid phases. It is seen that the amorphous sublayer consists only of several molecular layers. We note that the calculated thicknesses of the amorphous sublayer for

Table 1
The thickness of the formed amorphous sublayer on quenching of a 1-μm-thick melt layer on a copper backing

Material of melt	Al	Cu	Ni
h_g, nm	2.1	1.9	1,2

Table 2
The thermophysical and kinetic properties of the substance

Substance	Al	Cu	Ni	Fe
T_m, K	933	1356	1728	1530
$\rho^{(s)}/\rho^{(iq)}$, kg/m^3	2700/2370	8930/8030	8900/7790	7880/–
$\lambda^{(s)}/\lambda^{(iq)}$, W/(m K)	209/88	390/180	92/72	74/–
$c^{(s)}/c^{(iq)}$, J/(kg K)	880/1095	390/500	460/770	45/–
U, 10^{-20} J/atom	4.15	6.6	9.15	–
σ, J/m^2	0.093	0.18	0.255	–
L_v, 10^9 J/m^3	0.975	1.8	1.8	–
d_a, 10^{-10} m	2.6	2.3	2.3	–
K, m/(s K)	0.049	0.02	0.012	–

the quenched layers of thickness 1 and 10 μm were the same. This is due to the fact that the amorphization of the sublayer of the melt takes the times much smaller than the characteristic time of the passage of a heat wave over the thickness of the quenched layer, therefore the cooling rate of the melt near the backing over these times is virtually independent of the thickness of the quenched layer.

3. Spontaneous crystallization of the melt

3.1. Statement of the problem

In this section we consider the problem of spontaneous crystallization of a thin layer of the metal melt brought in contact with a semi-infinite backing. The z-axis with the origin on the free melt surface is directed into the depth of the backing. The boundary-value problem is written as follows.

The heat conduction equations for the layer of the melt and for the backing are:

$$\rho_m c_m \frac{\partial T_m}{\partial T} = \lambda_m \frac{\partial^2 T_m}{\partial z^2} + Q, \quad \rho_b c_b \frac{\partial T_b}{\partial T} = \lambda_b \frac{\partial^2 T_b}{\partial z^2}, \tag{5}$$

where $Q = \rho_m L \, d\eta/dt$ is the quantity of heat evolved in the process of crystallization by the centers of the new phase which originate spontaneously; L is the specific heat of melting of the melt substance, and η is the fraction of the crystalline mass in the melt.

The initial and boundary conditions are

$$T_m(0,z) = T_m^0, \quad T_b(0,z) = T_b^0,$$

$$T_m(t,h_m) = T_b(t,h_m), \quad \left(\lambda_m \frac{\partial T_m}{\partial z}\right)\Big|_{z=h_m} = \left(\lambda_b \frac{\partial T_b}{\partial z}\right)\Big|_{z=h_m},$$

$$\left(\frac{\partial T_m}{\partial z}\right)_{z=0} = 0, \quad (T_b)_{z\to\infty} = T_b^0. \tag{6}$$

Here we ignore heat exchange on the free surface of the melt and the thermal resistance of the forming amorphous sublayer, because of the relatively small thicknesses of the amorphous sublayer relative to the thicknesses of the quenched layer ($h_m \sim 1$ μm) which are considered in this work.

According to Kolmogorov's theory of the total kinetics of crystallization [14], the fraction of the crystalline mass in the melt η is determined as

$$\eta(t) = \frac{V(t)}{V} = 1 - \exp\left(-\frac{4\pi}{3} \int_0^t J(x) \left(\int_x^t v(x')\,dx' \right)^3 dx \right), \tag{7}$$

where V is the initial volume, $V(t)$ is the volume of the crystallized substance, and $v = K\Delta T$ is the rate of growth of a crystal. We note that, as it will be shown below, since the time of crystallization of the melt layer t_{cr} is much larger than the time of molecular relaxation, $t_{cr} \gg t_R$, in the calculations we use the stationary frequency of nucleation.

The number of crystallization centers N_c forming for the time t per unit volume is defined by the expression [14]

$$N_c(t) = \int_0^t J(x)(1-\eta(x))\,dx. \tag{8}$$

We introduce the following dimensionless variables: $\theta = T/T_m^0$, $\zeta = z/h_m$, and $\tau = a_m t/h_m^2$. Then the problem (5) and (6) can be written in the following form:

$$\frac{\partial \theta_m}{\partial \tau} = \frac{\partial^2 \theta_m}{\partial \zeta^2} + f(\tau,\zeta), \tag{9}$$

$$\frac{\partial \theta_b}{\partial \tau} = a_{b,m} \frac{\partial^2 \theta_b}{\partial \zeta^2}, \tag{10}$$

$$\theta_m(0,\zeta) = 1, \quad \theta_b(0,\zeta) = \theta_b^0, \tag{11}$$

$$\theta_m(\tau,1) = \theta_b(\tau,1), \quad \left(\frac{\partial \theta_m}{\partial \zeta}\right)_{\zeta=1} = \lambda_{b,m}\left(\frac{\partial \theta_b}{\partial \zeta}\right)_{\zeta=1}, \tag{12}$$

$$\left(\frac{\partial \theta_m}{\partial \zeta}\right)_{\zeta=0} = 0, \quad \theta_b(\tau,\zeta\to\infty) = \theta_b^0, \tag{13}$$

where $f(\tau,\zeta) = Ku\,\theta_{\mathrm{mel}}\,\mathrm{d}\eta/\mathrm{d}\tau$; $Ku = L/(c_{\mathrm{m}}T_{\mathrm{mel}})$ is the Kutateladze number; $\theta_{\mathrm{mel}} = T_{\mathrm{mel}}/T_{\mathrm{m}}^0$; $\theta_{\mathrm{b}}^0 = T_{\mathrm{b}}^0/T_{\mathrm{m}}^0$; $a_{\mathrm{b,m}} = a_{\mathrm{b}}/a_{\mathrm{m}}$; and $\lambda_{\mathrm{b,m}} = \lambda_{\mathrm{b}}/\lambda_{\mathrm{m}}$.

System (9)–(13) together with expressions (7) and (8) entirely determines the dynamics of crystallization and allows one to determine the microstructure of the solidified layer; i.e., to find the distribution of the medium crystallites over the layer thickness. This problem can be solved only numerically.

3.2. Numerical method of solution and the results

To construct a finite-difference scheme, we use the method of a control volume. We divide the time interval $[0,1]$ into M sublayers and the space interval $[0,1]$ into N sublayers. The section in the backing ζ_{b} where condition (13) is set is selected such that a heat wave for the time of complete solidification of the melt could not reach this section: $\zeta_{\mathrm{b}} - 1 \gg \sqrt{a_{\mathrm{b,m}}T_{\mathrm{cr}}}$, where $\tau_{\mathrm{cr}} = a_{\mathrm{m}}t_{\mathrm{cr}}/h_{\mathrm{m}}^2$. Assuming the steps over the coordinate ζ in the backing and in the melt to be equal, we obtain the relationship $N_1/N \gg \sqrt{a_{\mathrm{b,m}}T_{\mathrm{cr}}}$, where N_1 is the number of the nodes over ζ in the backing. The integral symbol i corresponds to the center of the spatial volume; the fractional symbols $i \pm 1/2$ correspond to its faces.

Integrating Eqs. (9) and (10) over the spatial–temporal volume $(\zeta_{i-1/2},\zeta_{i+1/2})$ (τ_j,τ_{j+1}) subject to the corresponding boundary conditions (12) and (13), we obtain the following system of the finite-difference equations:

for inner volumes

$$\left(\theta_{\mathrm{m}i}^{j+1} - \theta_{\mathrm{m}i}^{j}\right)M - \left(\theta_{\mathrm{m}i+1}^{j} - 2\theta_{\mathrm{m}i}^{j} + \theta_{\mathrm{m}i-1}^{j}\right)N^2 - f_i^j = 0 \quad (i = 2,\ldots,N-1),$$

$$\left(\theta_{\mathrm{b}i}^{j+1} - \theta_{\mathrm{b}i}^{j}\right)M - a_{\mathrm{b,m}}\left(\theta_{\mathrm{b}i+1}^{j} - 2\theta_{\mathrm{b}i}^{j} + \theta_{\mathrm{b}i-1}^{j}\right)N^2 = 0 \quad (i = N+2,\ldots,N+N_1-1);$$

for boundary volumes

$$\left(\theta_{\mathrm{m}1}^{j+1} - \theta_{\mathrm{m}1}^{j}\right)M - \left(\theta_{\mathrm{m}2}^{j} - \theta_{\mathrm{m}1}^{j}\right)N^2 - f_1^j = 0, \quad \theta_{\mathrm{b}N+N_1}^{j+1} = \theta_{\mathrm{b}}^0,$$

$$\left(\theta_{\mathrm{m}N}^{j+1} - \theta_{\mathrm{m}N}^{j}\right)M - \left(\theta_{\mathrm{m}N-1}^{j} - 3\theta_{\mathrm{m}N}^{j} + 2\theta_{\mathrm{m}N+1/2}^{j}\right)N^2 - f_N^j = 0,$$

$$\left(\theta_{\mathrm{b}N+1}^{j+1} - \theta_{\mathrm{b}N+1}^{j}\right)M - a_{\mathrm{b,m}}\left(\theta_{\mathrm{b}N+2}^{j} - 3\theta_{\mathrm{b}N+1}^{j} + 2\theta_{\mathrm{b}N+1/2}^{j}\right)N^2 = 0.$$

Initial conditions (11) take the form $\theta_{\mathrm{m}i}^0 = 1$, $\theta_{\mathrm{m}N+1/2}^0 = 1$, $\theta_{\mathrm{b}i}^0 = \theta_{\mathrm{b}}^0$, and $\theta_{\mathrm{b}N+1/2}^0 = \theta_{\mathrm{b}}^0$. It can be easily shown that for automatic satisfaction of conjugation conditions (12), it is necessary to comply with the condition

$$\theta_{\mathrm{m}N+1/2}^j = \theta_{\mathrm{b}N+1/2}^j = \frac{\theta_{\mathrm{m}N}^j + \lambda_{\mathrm{b,m}}\theta_{\mathrm{b}N+1}^j}{1+\lambda_{\mathrm{b,m}}} \quad (j = 1,M).$$

The specific feature of this problem is that in different sections of the layer crystallization occurs at different overcoolings. Consequently, the fraction of the crystalline phase and the number of the centers formed depend parametrically on ζ. Knowing the number of crystallization centers $N_{\mathrm{ci}}(t_{\mathrm{cr}})$ formed in the ith sublayer by the moment of complete solidification of the entire melt layer, it is possible to determine the mean radius of crystallites r_i in the given sublayer from the formula

$$r_{\mathrm{i}} = \left(\frac{3}{4\pi N_{\mathrm{ci}}(t_{\mathrm{cr}})}\right)^{1/3}$$

and thus to find the size distribution function $r(\zeta)$ of crystallites over the thickness of the entire layer.

To calculate the integrals in formulae (7) and (8), the formula of rectangles was used at each step of integration over the time. The minimum number of the divisions of the layer of the melt $N_{\min}$ was selected so that at the values $N = 2N_{\min}$ and $N = N_{\min}$ the calculations could coincide. This condition was satisfied, when $N = 10$–20. The values of N_1 varied within the limits $(50$–$100)N$. The time step was determined from the condition of stability for explicit schemes, $N^2/M < 1/2$ [15]. This condition was certainly satisfied at $M = 1000$.

The calculations were carried out for aluminum and copper layers of melts on various backings. The initial temperature of the melt in all of the calculations was assumed equal to the melting point of the melt substance: $T_{\mathrm{m}}^0 = T_{\mathrm{mel}}$, the initial temperature of the backing is $T_{\mathrm{b}}^0 = 300$ K. Table 2 lists the properties of the substances used in the calculations.

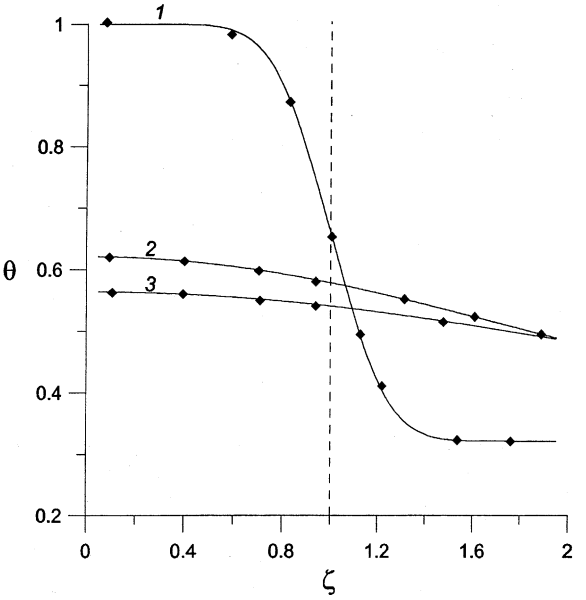

Fig. 1. Dynamics of the temperature field in cooling aluminum on an aluminum backing in the absence of solidification. Solid lines: analytical solution (4); points: numerical calculation: (1) $\tau = 0.02$; (2) $\tau = 1.46$; (3) $\tau = 2.32$.

Fig. 1 presents the results of the test numerical calculation of conjugate heat exchange of a layer of a melt and a backing in the absence of crystallization. It is seen that they agree well with the corresponding analytical solution (4).

Fig. 2a–c presents the results of numerical calculations which illustrate the dynamics of the temperature fields in the melts of aluminum on an aluminum and an iron backings and of copper on a copper backing, respectively. It is seen that intense heat release associated with the increase in the crystal mass leads to a substantial rearrangement of temperature fields. Thus, in the absence of crystallization, the temperature on the melt–backing interface by the time instant $\tau = 1.46$ decreases to 0.58 (see Fig. 1), whereas during crystallization by the same time instant it attains the value 0.72

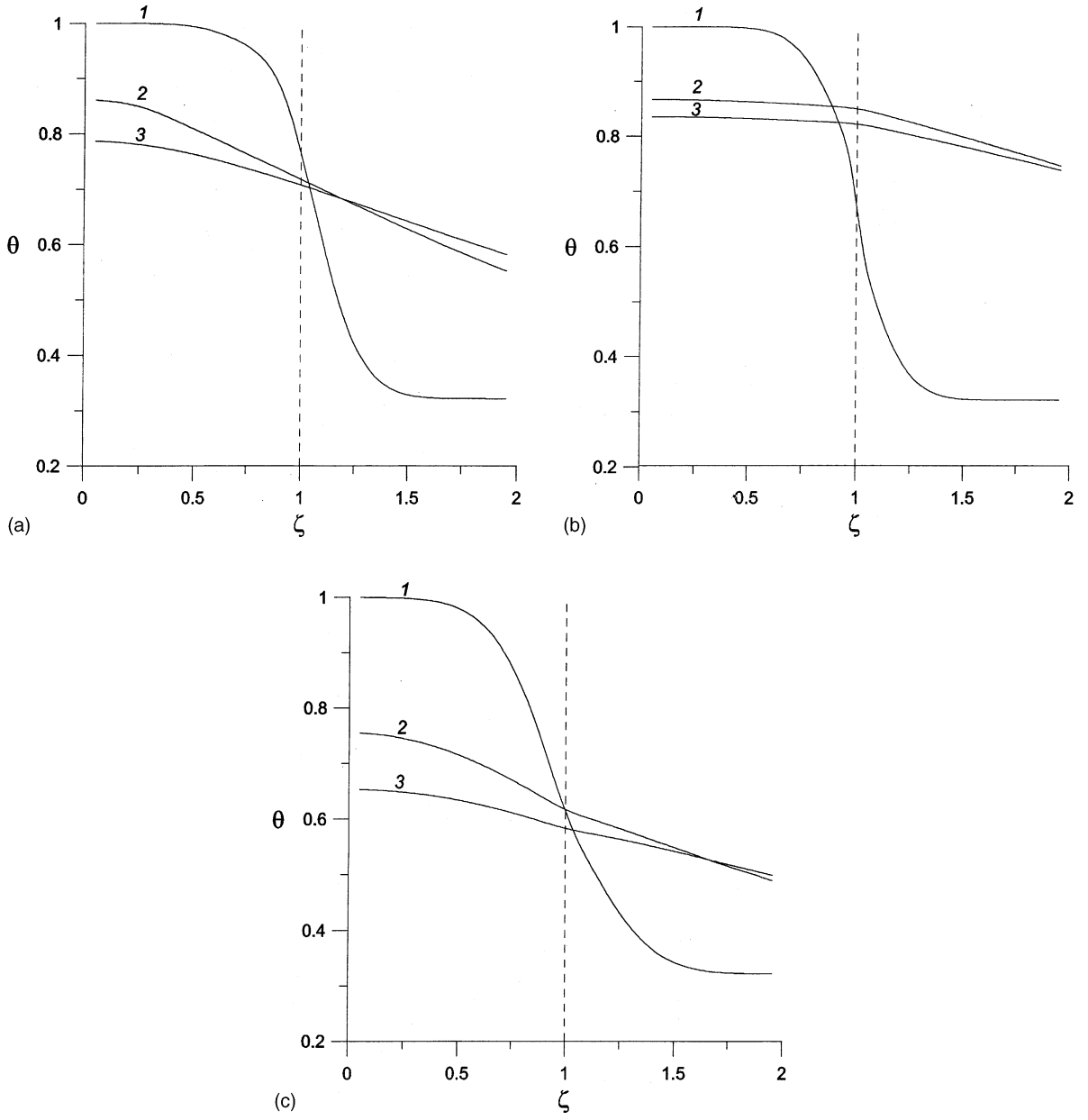

Fig. 2. The dynamics of the temperature field in crystallization: (a) of aluminum melt on an aluminum backing (1) $\tau = 0.02$; (2) $\tau = 1.46$; (3) $\tau = 2.32$; (b) of aluminum melt on an iron backing (1) $\tau = 0.02$; (2) $\tau = 5.65$; (3) $\tau = 6.71$; (c) of copper melt on the copper backing (1) $\tau = 0.04$; (2) $\tau = 1.37$; $\tau = 1.82$.

(see Fig. 2a). This substantial rise of the temperature is attributable to the large frequencies of nucleation and high value of the kinetic constant for aluminum. Precisely this property of aluminum explains its tendency to crystallize according to the equilibrium mechanism and the complexity in obtaining aluminum in an amorphous state [8]. It is seen from Fig. 2b that the relatively low thermal conductivity of an iron backing leads to a rapid decrease in overcooling and, consequently, to the approach of the solidification conditions to equilibrium ones. In contrast to aluminum, the melt of copper on a copper backing undergoes crystallization at very large overcoolings (see Fig. 2c), which are due to both the high thermal conductivity of the copper backing and the relatively low frequencies of nucleation in copper.

Fig. 3 demonstrates the dynamics of the increase in the fraction of the crystal mass in different sections of the layer of aluminum melt on an aluminum and an iron backings. It is seen that near the backing (in the section $\zeta = 0.85$) in both cases a plane crystallization front is immediately formed which remains plane for the aluminum backing up to the section $\zeta = 0.45$. For the iron backing, already in the section $\zeta = 0.65$, the crystallization front is not plane, since the increase in the fraction of the crystalline phase occurs over a considerable time interval from $\tau = 1$ to $\tau \simeq 2.5$. This is due to the intense release of heat because of the high nucleation frequency in the aluminum melt and the low heat-removing ability of the iron backing. Therefore, the duration of the aluminum melt solidification on an iron backing is almost twice the duration of solidification on the aluminum backing. An analysis of the dynamics of solidification of each sublayer allows the following conclusions to be drawn. At the start of the process, a crystallized mass is very small and increases slowly (a small number of growing crystallites and their small surface area). This time interval τ_i (see Fig. 3) is called the incubation period. Thereafter, the crystallization rate rises sharply and does not change until the volume of the uncrystallized substance is 10–20% of the initial one. This is accompanied by a rapid decrease in the initial overcooling, and the frequency of homogeneous nucleation decreases accordingly. This results in a decrease in the rate of the growth of the crystal mass.

The dependence of the time of complete crystallization t_{cr} on the parameter of the relative thermal activity K_e is presented in Fig. 4. Thus, on increase in K_e from 0.6 for the Al–Cu pair to 1.4 for the Al–Fe pair, i.e., by a factor of 2.3, the time of total solidification increases almost 3.8 times.

The proposed model made it possible to calculate the size distribution of crystallites over the cross-section of the layer quenched from its liquid state. For a 1-μm-thick aluminum layer on backings from Fe, Al, and Cu these data are given in Fig. 5. Schematically, the microcrystalline structure of the cross-section of the solidified layer, corresponding to curve 2 in Fig. 5, is shown in Fig. 6. In all of the three cases it is seen that with distance from the backing the mean size of the crystallites increases. This is attributed to the fact that at the initial time instant the maximum overcooling occurs over the thickness of the layer near the backing and,

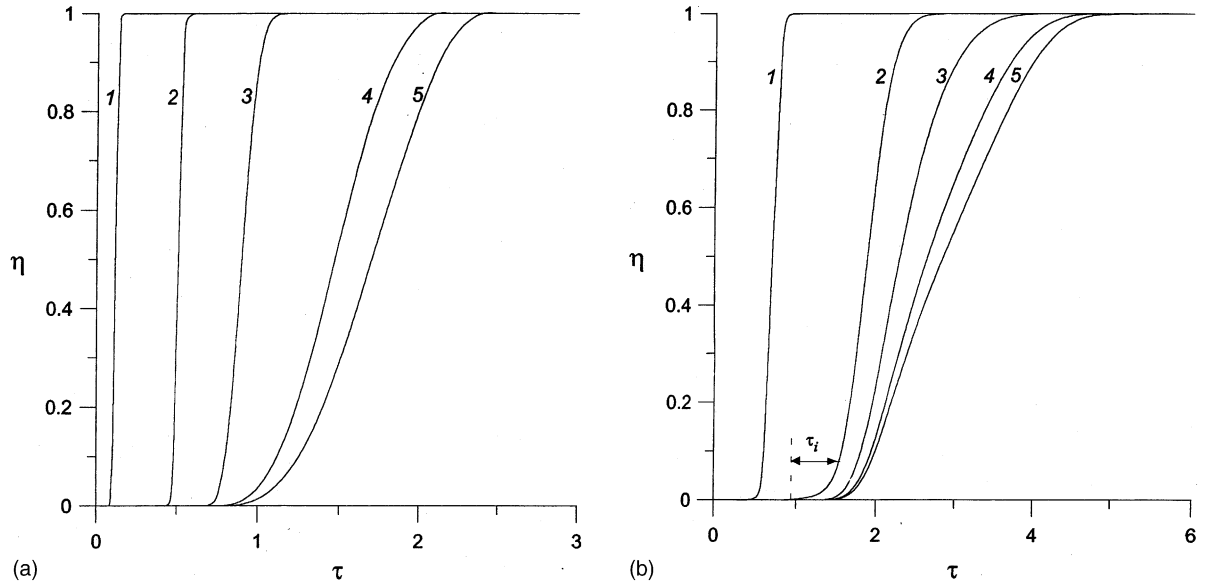

Fig. 3. Dependence of the fraction of a crystal mass on time in different sections of the aluminum layer: (a) on the aluminum backing; (b) on the iron backing; (1) $\zeta = 0.85$; (2) $\zeta = 0.65$; (3) $\zeta = 0.45$; (4) $\zeta = 0.25$; (5) $\zeta = 0.05$.

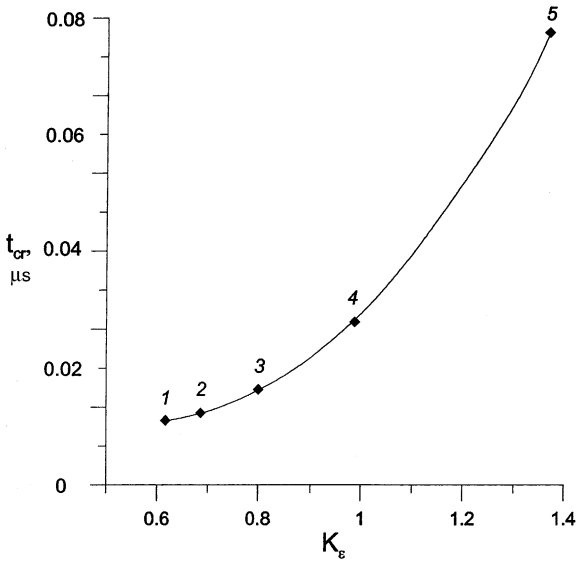

Fig. 4. Dependence of the time of complete solidification of the 1-μm-thick aluminum layer on the parameter of the relative thermal activity K_ε: (1) on the copper backing; (2) silver backing; (3) gold one; (4) aluminum one; (5) iron one.

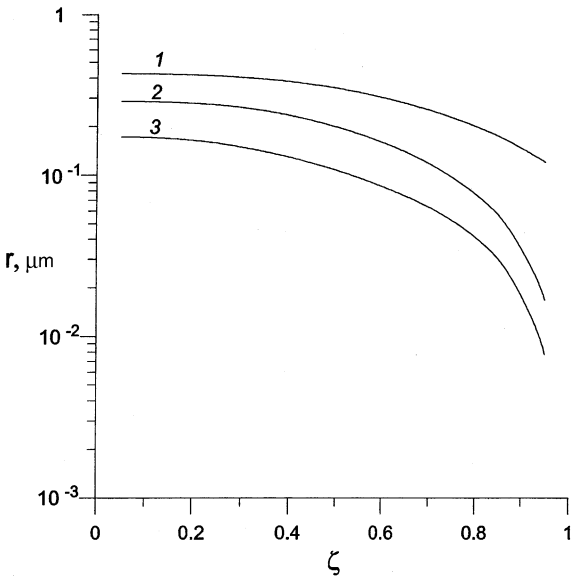

Fig. 5. Size distribution of crystallites over the thickness of the 1-μm-thick solidified aluminum layer on the backing made of: (1) iron; (2) aluminum; (3) copper.

consequently, the greatest nucleation frequency. Therefore, in the region adjacent to the backing a sharp increase in the crystal mass is observed in the initial moment. As the latent heat of phase change evolves, the

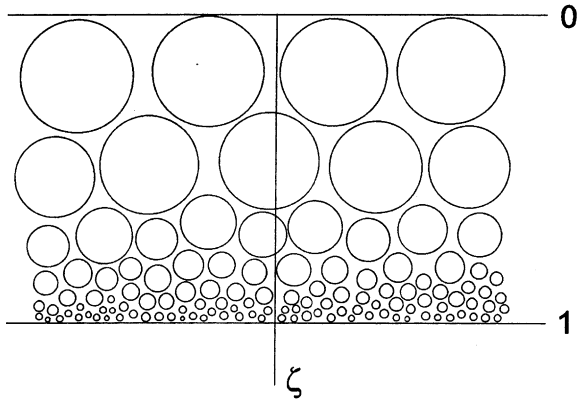

Fig. 6. Scheme of size distribution of crystallites over the thickness of the 1-μm-thick aluminum layer on the aluminum backing.

overcooling rapidly decreases and, correspondingly, the frequency of nucleation decreases, and the number of nuclei formed in the initial moment in this sublayer remains virtually the same up to the moment of complete solidification of the melt. A similar picture is observed for the regions located at a distance from the backing. But crystallization in them occurs at lower overcoolings than near the backing and, consequently, at smaller nucleation frequencies. This explains the inhomogeneousness of the structure of the layer quenched.

It also follows from the data obtained that the scatter of the values of r over the layer thickness decreases with increase in the parameter K_ε. Thus, by selecting the corresponding material for a backing it is possible to effectively control the microstructure of the solidifying layer, thus ensuring its sharp inhomogeneity in the case of backings with high thermal conductivity (curves 2 and 3 in Fig. 5) and also almost homogeneous distribution, when backings with low thermal conductivity are selected (curve 1 in Fig. 5).

4. Conclusions

The problem of solidification of a thin layer of melt brought into contact with a massive backing is considered. Based on the amorphization conditions formulated, the thickness of the amorphous sublayer formed on quenching near a backing has been determined which consists only of several molecular layers. A model of spontaneous crystallization of a melt is suggested which made it possible to find the size distribution of crystallites over the thickness of the solidified layer. The dependence of the degree of the inhomogeneity of the structure obtained on the thermophysical properties of a backing is shown.

References

[1] H. Herman (Ed.), Ultrarapid Quenching of Liquid Alloys, Treatise on Material Science and Technology, vol. 20, Academic Press, 1981.

[2] H.J. Gunterodt, H. Beck (Eds.), Glassy Metals. I. Topics in Applied Physics, vol. 46, Springer, Berlin, Heidelberg, New York, 1981.

[3] H. Jones, Splat cooling and metastable phases, Rep. Prog. Phys. 36 (11) (1973) 1425–1497.

[4] H. Jone, Rapid Solidification of Metals and Alloys, Institution of Metallurgists, London, 1982.

[5] H. Miura, S. Isa, K. Omuro, N. Tanigami, Production of amorphous based alloys by flame-spray quenching, Trans. Jpn. Inst. Met. 22 (9) (1981) 597–606.

[6] Yu.S. Borisov, V.N. Korzhik, Amorphous gas-thermal coatings: theory and experimental data, in: O.P. Solonenko, M.F. Zhukov (Eds.), Thermal Plasma and New Materials Technology. 2. Investigation and Design of Thermal Plasma Technologies, Cambridge Interscience Publishing, England, 1995, pp. 255–268.

[7] P. Chráska, J. Dubsky, B. Kolman and P. Raus, Phase changes during the plasma spray deposition in: O.P. Solonenko and A.I. Fedorchenko (Eds.), Plasma Jets in the Development of New Materials Technology, VSP, Utrecht, The Netherlands; Tokyo, Japan, 1990, pp. 311–320.

[8] A.I. Fedorchenko, Phase transition upon solidification from liquid state, J. Appl. Mech. Tech. Phys. 42 (1) (2001) 97–102.

[9] A.A. Chernov, A.I. Fedorchenko, A vitrification criterion for metal melts under hardening from the liquid state, Russian J. Eng. Thermophys. 19 (3) (2000) 201–206.

[10] I. Gutzow, J. Schmelzer, The Vitreous State Thermodynamics, Structure, Rheology and Crystallization, Springer, Berlin, 1995.

[11] V.I. Motorin, Vitrification kinetics of pure metals, Phys. Status Solidi 80A (1983) 447–455.

[12] Ya.B. Zel'dovich, Toward the theory of formation of a new phase. Cavitation, Zh. Eksp. Teor. Fiz. 12 (11–12) (1942) 525–538.

[13] A.V. Luikov, Heat Conduction Theory, Izd. Vyssh. Shkola, Moscow, 1967.

[14] A.N. Kolmogorov, On statistical theory of metal crystallization, Izvestiya Acad. Sci. USSR. Ser. Mathem. 1 (1937) 355–359.

[15] P.J. Roache, Computational Fluid Dynamics, Hermosa Publishers, Albuquerque, New Mexico, 1976.